University of Plymouth

PEARL **https://pearl.plymouth.ac.uk**

Faculty of Science and Engineering School of Biological and Marine Sciences

2015-05-15

The role of advection in the distribution of plankton populations at a moored 1-D coastal observatory

Cross, J

http://hdl.handle.net/10026.1/3760

10.1016/j.pocean.2015.04.016
PROGRESS IN OCEANOGRAPHY
Elsevier BV

All content in PEARL is protected by copyright law. Author manuscripts are made available in accordance with publisher policies. Please cite only the published version using the details provided on the item record or document. In the absence of an open licence (e.g. Creative Commons), permissions for further reuse of content should be sought from the publisher or author.

*Manuscript
Click here to view linked References

The role of advection in the distribution of plankton populations at a moored 1-D coastal observatory

Jaimie Cross[a,*], W. Alex M. Nimmo-Smith[a], Philip J. Hosegood[a], Ricardo Torres[b]

[a] *School of Marine Science and Engineering, Plymouth University, Drake Circus, Plymouth PL4 8AA, UK*
[b] *Plymouth Marine Laboratory, Prospect Place, The Hoe, Plymouth PL1 3DH, UK*

Abstract

The degree to which advection modulates the distribution of plankton populations at a 1-D coastal observatory was assessed at station L4 in the western English Channel (50° 15′ N 4° 13′ W, depth 50 m), part of the Western Channel Observatory (WCO). Five tidal-cycle surveys were conducted, three in spring and two in summer 2010. Observations of the physical characteristics of L4 were obtained by using a moored acoustic doppler current profiler (ADCP) and a free-falling microstructure sensor (MSS). The moored ADCP highlighted the presence of vertical shear, with typical values of U during spring tides of $\sim$ 0.5 m s^{-1} at the surface and $\sim$ 0.2 m s^{-1} at the bed. The distribution of phyto- and zooplankton populations above a size threshold of 200 μm were examined using an in-line holographic imaging system, the Holocam. Variability in time as well as depth is a common feature throughout each of the surveys, with examples of recorded numbers of phytoplankton that ranged between 1300 L^{-1} and 2300 L^{-1} at the same depth but at different points within the tidal cycle. Further, at the same points in the tidal cycle the number of recorded zooplankton was also seen to vary, specifically with

*Corresponding author. 3a Reynolds Building, Drake Circus, Plymouth University, Plymouth PL4 8AA UK
Email address: jaimie.cross@plymouth.ac.uk (Jaimie Cross)

the identification of gelatinous planula in spring that increased the observed number to maximums of between 140 L^{-1} and 220 L^{-1} in the upper layer, considerably higher that the corresponding WP-2 net counts for a similar period. Specific aspects of the movement and transfer of plankton relating to advection and interaction with the pycnocline are identified, both across tidal cycles and seasons.

Keywords: Shear; Advection; L4; Plankton dispersal; Holographic imaging; Potential Energy Anomaly; WCO; Western English Channel

1. Introduction

The distribution of plankton populations in shelf and coastal regions is of major importance in our effort to better understand carbon cycling and the temporal and spatial variability of the so-called 'biological pump'. Shelf seas in particular are disproportionate contributors to the export of carbon from the atmosphere to the deep ocean, accounting for $>40\%$ of the global total (Jahnke, 2010). Phytoplankton play a direct role in the uptake of dissolved inorganic carbon (DIC), whilst zooplankton have equal importance within the carbon cycle as consumers of phytoplankton and supporting both marine ecosystem dynamics and fisheries activity (Caley et al., 1996).

Quantifying the distribution of plankton populations in energetic, coastal environments offers a considerable challenge. Typically, multi-disciplinary studies that would take into account plankton dynamics are logistically challenging, requiring a suite of instrumentation that is frequently unavailable or expensive to operate both in time and finance. Often, measurements of fluorescence and optical backscatter (OBS) are taken along with *in situ* water samples to provide insight into the movement and transfer of plankton (e.g. Corcoran and Shipe 2011). Relative measures of OBS and fluorescence are insufficient, however, when needing to confidently supply quantitative information concerning biomass, plankton concentration or number. Determining the composition and structure of plankton populations *in situ* poses

an even greater challenge, particularly as most, if not all available methods to determine distribution rely on disturbing plankton from their natural environment (e.g. the Optical Plankton Counter (Herman et al., 2004), and the submersible FlowCam (See et al., 2005)).

The application of an *in situ* instrument that does not directly interfere with its sample, the Laser in situ Scattering and Transmissometer (LISST) more commonly used for investigations into suspended particulate matter, is growing in popularity amongst phytoplankton ecologists (Rzadkowolski and Thornton, 2012). However, the LISST has been recently shown to be unreliable when attempting to quantify non-spherical natural particulates (Davies et al., 2012; Graham et al., 2012). As such, when using this instrument to evaluate changes to the distribution of plankton, it is unclear whether the LISST is the appropriate tool in light of the range of shapes exhibited by plankton in the natural environment (McCandliss et al., 2002; Karp-Boss et al., 2007). As demonstrated recently by Cross et al. (2013), the emerging technology of holographic imaging offers the benefit of *in situ*, non-destructive sampling of the water column, and is used exclusively throughout this work to enumerate plankton populations. The flexibility afforded by holographic imaging allows for the simultaneous analysis of both phyto- and zooplankton distributions.

The Western Channel Observatory (WCO), maintained and run by Plymouth Marine Laboratory (PML), is located in the Western English Channel and includes a permanent station, L4, where long-term oceanographic and biogeochemical observations have been routinely collected on a weekly basis since 2002 (available from the WCO website at http://www.westernchannelobservatory.org.uk/data.php), which supplement further historical plankton records collected since the late 1980s (Figure 1). Much of the focus of the research at this location has involved long-term characteristics of biological particle populations, rarely invoking physical forcing as the principal driver of change (e.g. Widdicombe et al., 2010). Build-

ing on the short-term temporal variability of physical forcing at L4 brought about by the presence of vertical shear highlighted by Cross et al. (2014), such variability is invoked as the principle driver of the observed changes throughout each of the surveys presented in this work. The identification of advection as being a potentially important contributor to the structure of the water column at L4 could hold consequences for the measurement of plankton populations at this and other similar locations, given the likelihood of such populations to be substantially altered by sheared flow. The principal aim of this paper then, is to apply a novel method to help quantify and explain the degree to which the accurate sampling of plankton populations might be impacted by tidal advection, and also to examine how these populations might change across the spring-neap cycle and seasons.

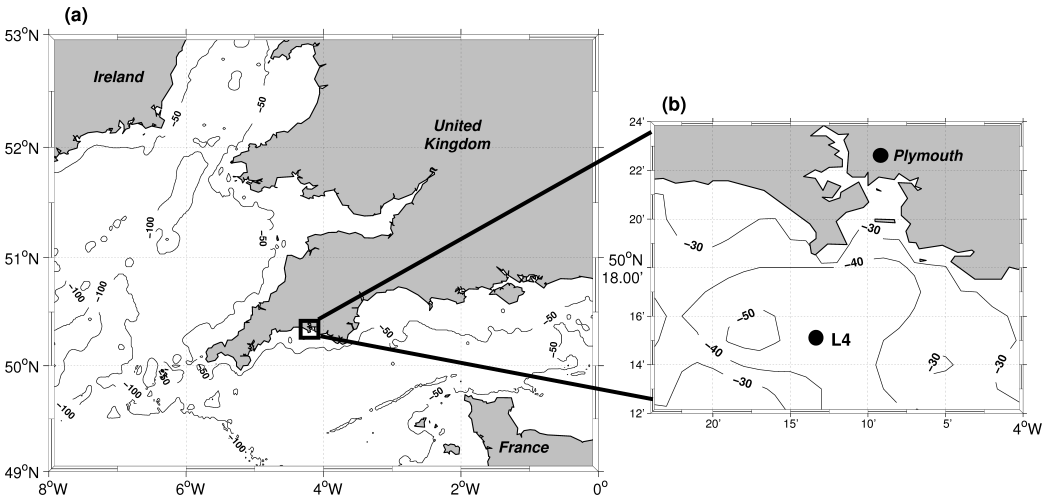

Figure 1: Map of the southern part of the United Kingdom (a) with exploded section noting the location of Station L4, approximately 10 km south of Plymouth (b)

2. Methods

2.1. Survey location

Station L4 resides approximately 10 km south of Plymouth at 50° 15′ N 4° 13′ W where the water depth is around 50 m with a seabed predominantly

consisting of sand. Long-term data exist for temperature and salinity at L4, in addition to phytoplankton and zooplankton abundance, and forms a central part of the WCO. The long-term data indicates that the site is well-mixed during the winter, and weakly stratified between April and October. When stratified, the water column has an average difference in temperature of 2 °C between the upper and lower layers (Cross, 2012). The site is characterised by a dominant semi-diurnal tide, experiencing a maximum range of over 5 m that generates currents of 0.5-0.6 m s^{-1} at the surface.

2.2. Physical measurements

2.2.1. The Lagrangian surveys

Measurements utilising an array of instruments were undertaken during five surveys in spring and summer 2010 aboard the *RV Plymouth Quest*. Instruments were deployed in a Lagrangian reference frame whilst following a drifter drogued by a holey sock positioned at 3-12 m. Within the drifter-drogue assembly, a downward-facing 600 kHz Acoustic Doppler Current Profiler (ADCP) was fixed within a neutrally-buoyant submersible at an approximate depth of 20 m. The ADCP sampled at 2 s intervals with a bin size of 0.5 m, with the depth of the first good bin at 21 m. The device was able to resolve the level of current shear present for the lower part of the water column. The vessel relocated to the drifter each hour, and measurements were obtained whilst the drifter was no further than 100 m from the ship. A free-fall microstructure profiler, the ISW Wassermesstechnik MSS-90, was utilised to observe the turbulent velocity shear. The number of profiles taken during each hour ranged from 6-8. The MSS-90 contains a number of sensors including optical backscatter (OBS), a fluorometer and conductivity, temperature and depth (CTD) probe. The dissipation rate of turbulent kinetic energy was estimated from the small-scale shear and assuming isotropy is defined as:

$$\varepsilon = 7.5\nu\langle(\partial u/\partial z)^2\rangle, \tag{1}$$

where ν is the kinematic viscosity, which in seawater takes the value of about $10^{-6}\,\mathrm{m^2\,s^{-1}}$, and $\partial u/\partial z$ represents the spatial derivative of the horizontal current component, u, in the vertical direction, z. The angled brackets denote a suitable time average, and the units of turbulent dissipation are given in $\mathrm{W\,kg^{-1}}$. MSS-90 profiles begin at a depth of 5 m, due to the potential for contamination from the motion of the boat induced by wave activity (Lozovatsky et al., 2006). The MSS-90 samples at a rate of 1024 Hz with a typical fall speed of $0.5\,\mathrm{m\,s^{-1}}$. Such high frequency measurements allow for great confidence in the estimate of ε.

2.3. Holographic camera

An in-line digital holographic imaging system, the Holocam, was also deployed. The Holocam is mounted on a steel frame along with a CTD, and is described fully in Graham and Nimmo Smith (2010). Briefly, the system contains a laser light source that illuminates a sample volume containing plankton particles which scatter the light, whereupon an interference pattern is generated and subsequently recorded by a charge-coupled device (CCD). The resulting hologram is then computationally reconstructed post-deployment to give in-focus images of every particle in the sample volume, allowing for the calculation of particle statistics such as volume concentration and size distribution. Each raw hologram has a pixel resolution of 4.4 μm, and is 1536 x 1024 pixels in size, yielding a sample volume of $1.65\,\mathrm{cm^3}$ which is later scaled up to one litre during post-processing. In practical terms the minimum particle size resolved by this system is around 25 μm, with the maximum size limited only by the size of the CCD, here in excess of 6 mm. The Holocam was profiled vertically through the water column once each hour, near-simultaneously with the MSS profiles. The sampling frequency was 5 Hz with a profiling speed typically in the range of 0.2-0.4 $\mathrm{m\,s^{-1}}$, thus samples were obtained at a vertical resolution of around 5-6 cm.

The average number of holograms taken during a given profile of the instrument is around 1000; however the number of images for a given section

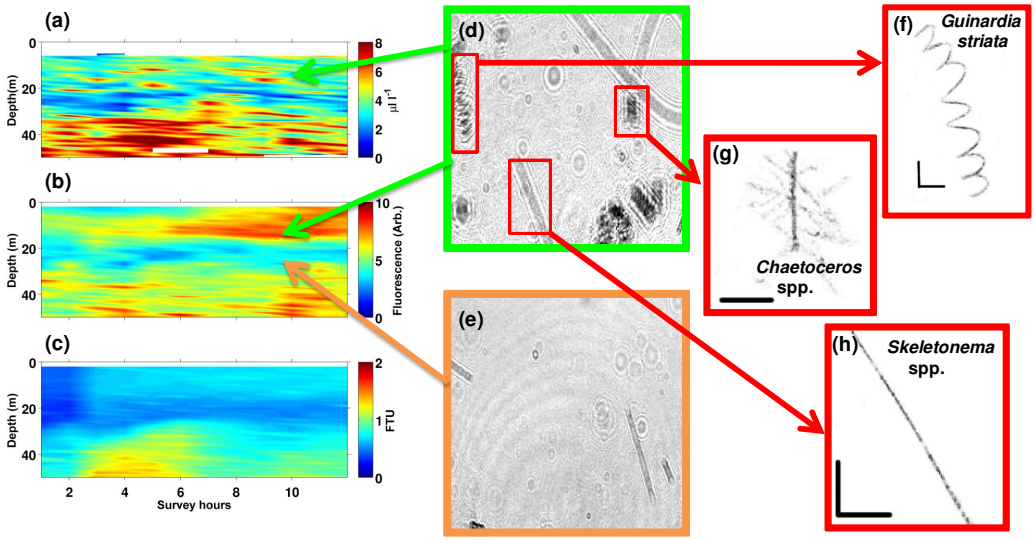

Figure 2: Illustration of the initial particle analysis using signals of interest from the MSS. Part (a) shows the total particle volume concentration (Holocam), (b) and (c) the response from the fluorescence and OBS sensors (MSS). Parts (d) to (h) represent a step-wise view of selecting raw holograms prior to numerical reconstruction in order to establish the type of plankton present. The scale bar in (f) is 200 μm, in (g) and (h) 100 μm.

of the water column may vary with the minor variation in fall speed range or water column properties. With the sample volume of each image, the total volume of water sampled during each profile would be in the region of 1.5-2 L. An illustration of how the Holocam is used to assess the particle environment is further displayed in Figure 2. The first step of this analysis is to locate the raw holograms that relate to the area of the water column that is of interest. Regions of interest (ROI) may be defined within each hologram and numerically reconstructed, revealing a sharp and in-focus image of planktonic particles (Figure 2f to h).

An additional technique was employed to determine how plankton may be altered by changes to their physical environment, and also where within a tidal cycle their number is shown to vary. Prior to this work, such enumeration of plankton has not been possible *in situ* without disturbing the plankton from their natural environment. Within the size range of phyto-

plankton that the Holocam may reliably resolve, phytoplankton biomass at L4 is dominated by chain-forming phytoplankton (Widdicombe et al., 2010), whereby within each image a colony of multiple diatom cells is regarded a single suspended particle. Diatom chains are routinely found to grow to several mm in size and are readily identifiable from the image data. However, to maximise efficiency when counting individual colonies, only phytoplankton $\geq 200\,\mu$m were identified and recorded. The assumption is made that this threshold would be sufficient to identify changes to the phytoplankton population brought about by changes imposed upon the water column by physical processes.

A simple, graphical user interface was designed in Matlab which took a flattened, reconstructed image of a 1024 x 1024 ROI as an input. Blocks of images were collated within 5 m intervals. Plankton were first identified as present through simple observation of each image. Upon identification, selection of the plankton was achieved through the click of a computer mouse. The interface stored each click as a single piece of plankton, allowing for the calculation of the mean number of plankton per unit volume of 1 L. Throughout this paper, the term number is used to refer to this metric when describing changes to both the phyto- and zooplankton populations.

2.3.1. Bedframe deployment

In addition to the Lagrangian surveys, a further deployment of a moored ADCP was conducted for a two-week period from 28th July 2010 to August 11th 2010. Deployments were also scheduled for the spring and autumn seasons but were thwarted by logistical challenges. An upward-facing 600 kHz ADCP was placed within a bedframe at the seabed. The ADCP sampled at 6 s intervals with a bin size of 1 m, with the first good bin at a height of 2 m above the bottom (mab). Despite the lack of seasonal coverage, the ADCP data would provide the background context with respect to the properties of the current and also clearly demonstrates the degree to which shear is present at L4.

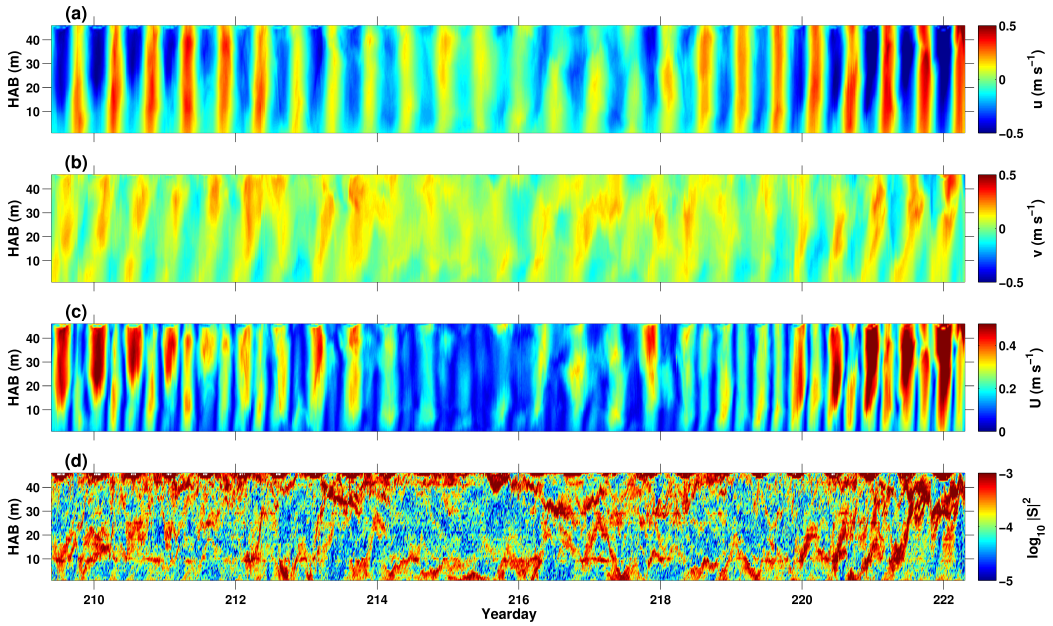

Figure 3: Results from the moored ADCP deployed at L4 during summer 2010. Plots (a) and (b) display the u and v components of velocity, (c) the velocity magnitude, U, and (d) shear, $|\mathrm{S}|^2\,(\mathrm{s}^{-2})$. HAB refers to height above the bottom.

3. Results

3.1. ADCP deployment summer 2010

Placing the Lagrangian surveys into context the deployment of the moored ADCP showed, for summer at least, that the water column at L4 is subjected to varying degrees of current shear (Figure 3c). The tidal current at L4 is dominated by the east-west, or u component with speeds frequently reaching $0.5\,\mathrm{m\,s^{-1}}$ toward the surface during spring tides, and occasionally exceeding this toward the latter part of the deployment. Neap tides, occurring during the middle of the deployment typically yield lower maximum values of around $0.3\,\mathrm{m\,s^{-1}}$ toward the surface. Shear is calculated as $|\mathrm{S}|^2 = \sqrt{\left(\frac{\partial u}{\partial z}\right)^2 + \left(\frac{\partial v}{\partial z}\right)^2}$, with the logged values displayed in (Figure 3d). The entire deployment of the bedframe is characterised by patches of elevated $|\mathrm{S}|^2$ that frequently exceed $10^{-3}\,\mathrm{s^{-2}}$ largely toward the surface and closer to the bed, with values in the

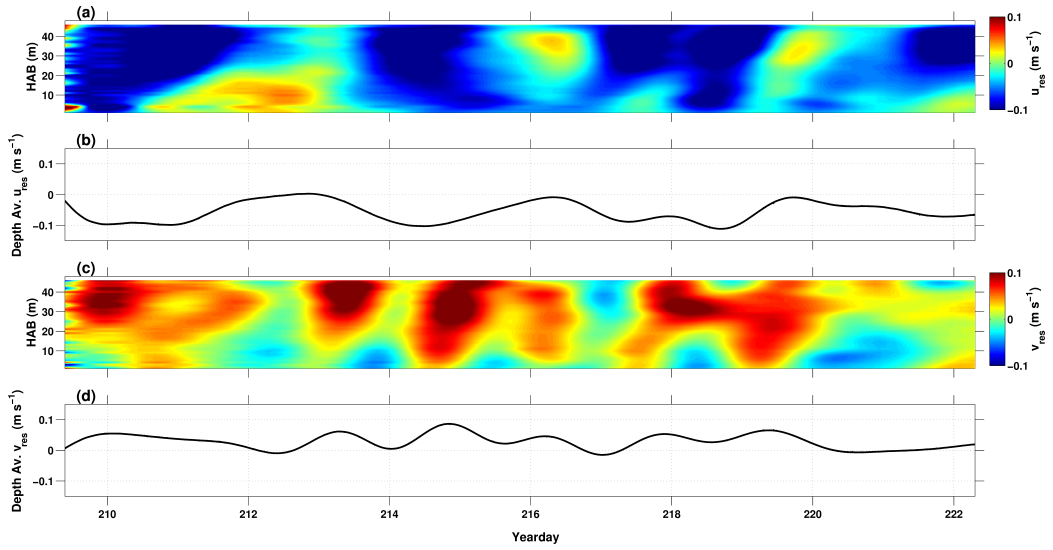

Figure 4: Mean flow at L4 during the bedframe deployment. Plots (a) and (c) show the residual velocity in the u and v directions respectively. The depth-averaged velocity values for each component are displayed in (b) and (d).

middle of the water column an order of magnitude lower. These lower values are more often present during the periods when U is reduced, particularly during neap tides. The general picture presented by the calculated $|\mathrm{S}|^2$ is of a site that is regularly exposed to persistent and high levels of sheared flow.

Residual flow is determined by low-pass filtering of the tidal signal with a 0.75 cycles day^{-1} (cpd) cut-off, yielding the values displayed in Figure 4. As anticipated for this site, the dominant flow is along the west-east (u) axis, with values of this component frequently approaching 0.1 m s^{-1} and directed predominantly to the west. North-south, or flow in the v direction is broadly 50% weaker, predominantly directed to the north. However, the deployment period is short, and likely to be impacted by rapid changes to the meteorological conditions that are occasionally observed. Periods of increased wind forcing are experienced during this deployment, which could influence the direction of the residual flow (e.g. see later Figure 7). The example of the week 5 observations on the 4th August and the days preceeding demonstrate

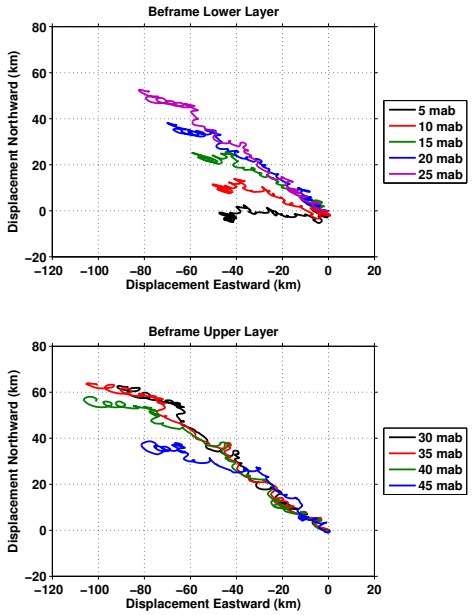

Figure 5: Progressive vector diagrams from the deployment of the moored ADCP. The water column is split into upper and lower layers as labelled, further highlighting the presence of sheared flow.

this whereby the wind was directed from the south, likely influencing the direction of the net flow which is pushed to the north at this time. Whilst these values offer an indication of the residual flow at this site, it is clear that a future deployment of greater duration would benefit all users of L4.

A further illustration of the vertical shear that dominates the dynamics of the water column at L4 is given by a progressive vector diagram (Figure 5). Broadly, the water column can be split into two layers, the lower ~ 20 m. and upper ~ 30 m. The mean displacement for a given water particle for the lower layer is 61 km on a broad heading of west-north-west. In contrast, for the upper layer the mean displacement is 99 km directed to the north-west.

3.2. Background meteorological data for the tidal surveys

Meteorological observations throughout the period of the spring surveys are shown in Figure 6. The Plymouth University meteorological station pro-

vided the observed wind stress, τ, rainfall and air temperature. Winds were light throughout April 2010, during the survey period yielding a maximum value for τ of $0.2\,\mathrm{N\,m^{-2}}$ between weeks 1 and 2. The wind stress presented in plot (a) of Figure 6 indicates that the potential for wind stirring, and therefore enhanced episodes of turbulent events at the surface, was reduced, particularly during the dates of the measurement campaigns. Similarly, the level of precipitation was very low during this month and once again on the dates of each of the surveys no rainfall was recorded by the met station nor experienced on board the vessel during the deployment. There was a gradual increase in air temperature in April, the mean air temperature during week one was 8.8 °C compared with 13.2 °C during week 3 (Figure 6b-c). The observed sea surface temperature (SST) reflects the increase in air temperature with a mean value of 9.2 °C during week 1 and 10.3 °C for week 3. There are several missing periods from instances when the L4 buoy was offline which have been supplemented by satellite from the AVHRR pathfinder dataset. Further limitations with respect to SST came from the amount of cloud cover present.

A measure of the extent to which the meteorological parameters influence the stability of the water column is the buoyancy flux, J_b. Positive values of J_b indicate stabilising conditions and *vice versa*. Following Hosegood et al. (2008), the buoyancy flux is given by

$$J_b = c_p^{-1} g \rho^{-1} \alpha Q + g \rho^{-1} \beta (E - P) S_{surf} \tag{2}$$

in units of $\mathrm{W\,kg^{-1}}$. Here, $Q = Q_{shortwave} + Q_{longwave} + Q_{latent} + Q_{sensible}$ which represents the total heat flux ($\mathrm{W\,m^{-2}}$) , c_p is the specific heat of water and g the acceleration due to gravity. Evaporation and precipitation are given by E and P respectively, S_{surf} is the surface salinity, with α and β representing the thermal expansion and haline contraction coefficients. It should be noted that the gaps that appear in Figure 6c represent periods where the lack of both SST and S_{surf} meant that J_b could not be computed, and that for days

111 to 115 a constant S_{surf} value was required. The terms that dominate J_b are $Q_{shortwave}$ and Q_{latent}, whereby short wave radiation stabilises and the latent heat flux acts to destabilise during periods of strong winds. In the absence of the latter, the general pattern is one of stability with daily maximums of J_b frequently exceeding $5\,\mathrm{x}\,10^{-7}$ W kg^{-1}. The largely negative value of J_b during day 104 can be attributed to the lack of solar insolation through increased cloud cover and low air temperature.

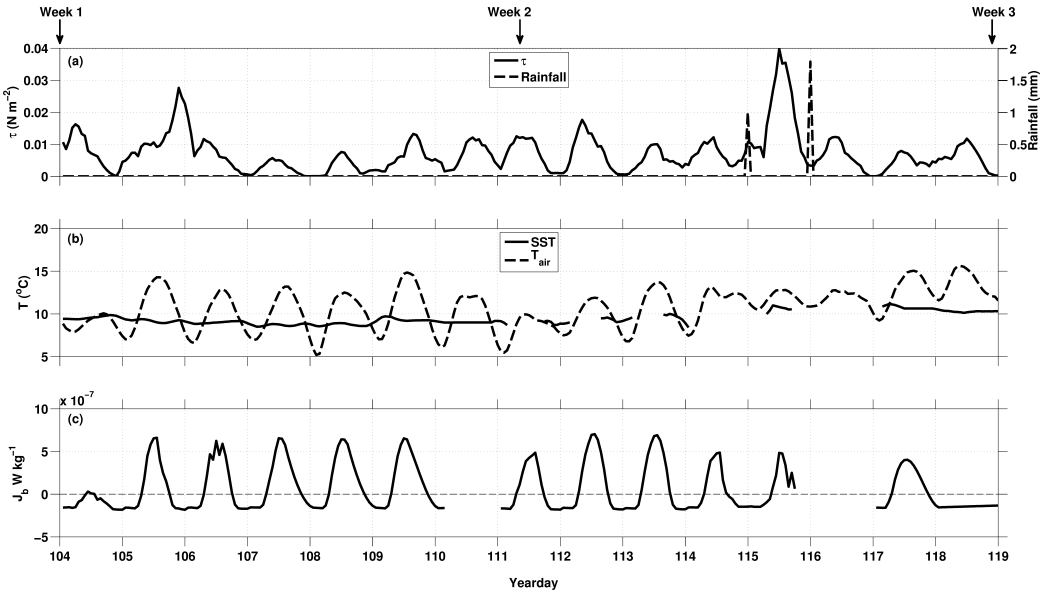

Figure 6: The background meteorological data for the survey period during generated by observations from the PU met station. Plot (a) displays wind stress (τ) and rainfall, (b) air and sea surface temperature, and (c) buoyancy flux (J_b). Both (a) and (b) consist of daily averages. With respect to SST, limited data was available due to the L4 buoy being off-line. Satellite data were used where possible but was also limited due to the presence of cloud-cover. The arrows mark the positions of each of the survey periods.

The planned surveys of weeks 4 and 5 were each due to be conducted across 12 hours, in the same manner of those in April, however the meteorological conditions experienced throughout these campaigns did not allow for this. The impact of these conditions can be considered in addition to the relative change imparted by seasonal elements such as increased insolation.

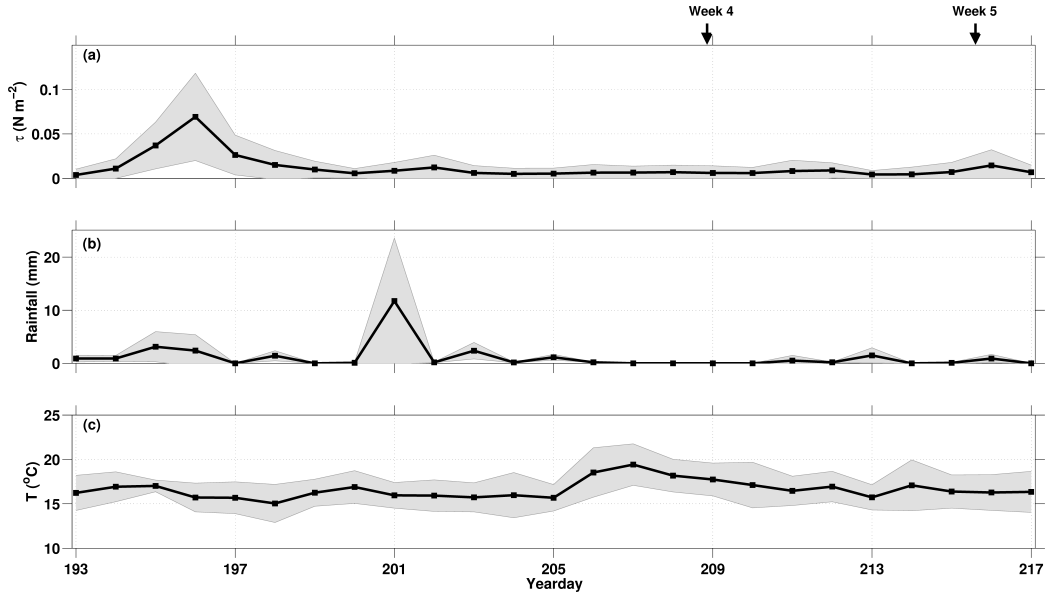

Figure 7: The background meteorological data for the survey period of weeks 4 and 5 generated by observations from the PU met station. Plot (a) displays wind stress (τ), (b) rainfall and (c) air temperature. All plots consist of daily averages, with the shaded region representing 1 S.D about the mean.

By way of context, some of the key meteorological parameters are displayed in Figure 7. Unfortunately, the calculation of the buoyancy flux could not be achieved across this period due to the absence of SST and sea surface salinity (SSS) measurements. The L4 buoy would ordinarily supply this data but was off-line from the 30th July for a period of around one month. Additionally, the satellite data that was used to provide supplementary data as per the previous weeks were not available due to the extent of the cloud cover.

3.3. Spring 2010 surveys

The evolution of several of the measured parameters for each survey is displayed in Figures 8 and 9. Spring tides occurred during weeks 1 and 3 with neaps in week 2 when the minimum tidal range was experienced ($\approx$2 m). Each of the plots displays observations across a 12 hour tidal cycle observed

in weeks 1, 2 and 3 respectively.

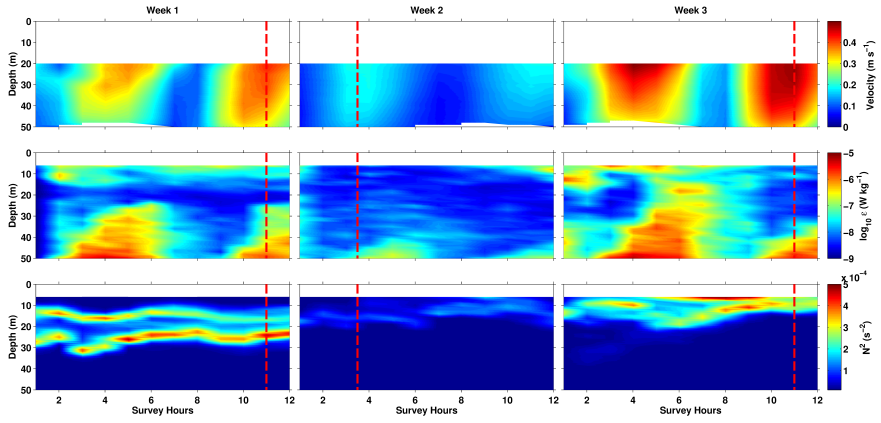

Figure 8: Measurements obtained from the ADCP and MSS for each of the surveys. The uppermost row displays the velocity magnitude observed with the ADCP. The middle row contains the dissipation of turbulent kinetic energy, ε, with the bottom row showing the buoyancy frequency, N^2. The vertical dashed lines mark the point of high water for each survey.

During week 1, the peaks in ε occur shortly after the times of peak flow, whereby the maximum velocities recorded by the ADCP are $0.37\,\mathrm{m\,s^{-1}}$ and $0.42\,\mathrm{m\,s^{-1}}$ for the ebb and flood tides respectively. Maximum values for ε are experienced between hours four and five, with values approaching 10^{-5} $\mathrm{W\,kg^{-1}}$ at the seabed. Enhanced dissipation at the bed is broadly coincident with the peaks in U, though the largest values for ε occur around 1-1.5 hours following the periods of faster current velocity. The influence of the pycnocline on ε is evident, apparently suppressing turbulent activity where values for N^2 are in excess of $10^{-4}\,\mathrm{s^{-1}}$ at around 15-30 m. This is also reflected in the plots of salinity and density, but to a lesser extent in temperature, illustrating the greater influence of salinity on the water column than temperature for this survey. This is reflected in the density ratio, a parameter that quantifies the relative influence of temperature and salinity on density,

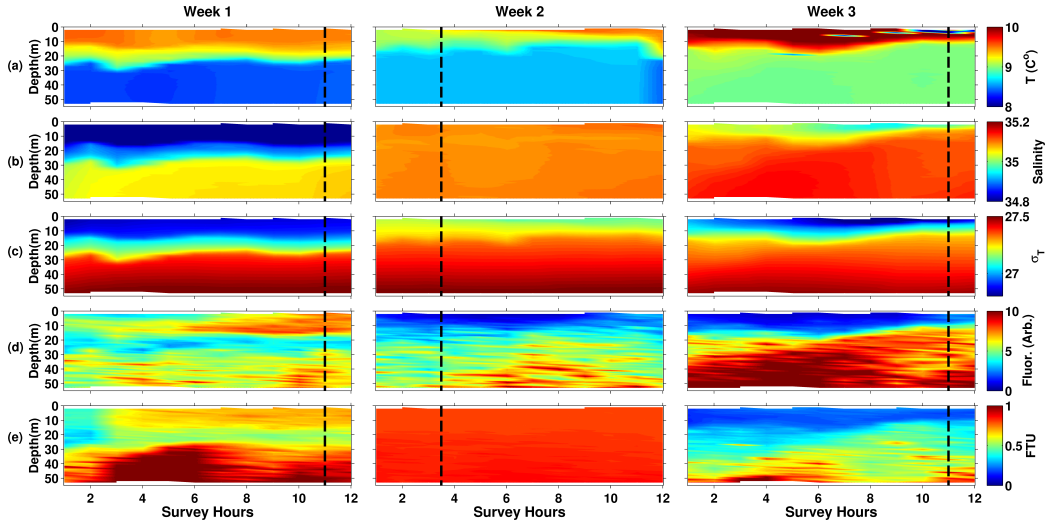

Figure 9: Scalar parameters obtained from the MSS measurements. The top row (a) displays temperature, followed by salinity (row b) and *in situ* density (row c). rows (d) and (e) shows fluorescence and turbidity respectively for each of the surveys as labeled. The vertical dashed lines mark the point of high water for each survey.

where values within the range of -1 to 1 indicate a dominance of salinity and is expressed as

$$R_\rho = \frac{\alpha(\Delta T)}{\beta(\Delta S)} \tag{3}$$

where, as previously, α and β are the thermal expansion and haline contraction coefficients respectively. For this week, the mean $R_\rho = -0.68$ in the upper 25 m of the water column.

The markedly reduced values for ε during week 2 are illustrative of the reduced flow experienced during neap tides. Current velocities were observed to be $< 0.2 \mathrm{m\,s^{-1}}$ for both ebb and flood, reflected in maximum dissipation around 10^{-6} $\mathrm{W\,kg^{-1}}$ in the bottom 3 m of the water column. There is a more marked time-velocity asymmetry when compared with either week 1 or week 3. The lower values of dissipation are evident and decrease to values approaching 10^{-8} $\mathrm{W\,kg^{-1}}$ at a depth of around 40 m throughout the survey. The apparent absence of stratification in week 2 is consistent with the

corresponding plots for turbulent dissipation, although a weak pycnocline does exist during this time, with N^2=$10^{-6}\,\mathrm{s}^{-2}$ at numerous points. Further temporal variability is displayed in week 3. Elevated levels of ε return as a consequence of the spring tides, with increased tidal velocities of close to $0.5\,\mathrm{m\,s}^{-1}$ during both high and low water generated by a larger tidal range ($>3\,\mathrm{m}$). This results in enhanced values of dissipation which more readily exceed 10^{-5} $\mathrm{W\,kg}^{-1}$, and higher values of 10^{-4} $\mathrm{W\,kg}^{-1}$ are not uncommon, particularly within the bottom 5 m of the water column. The pycnocline is shallower here at around 10-20 m and seemingly it is temperature that controls the water column with the mean $R_\rho = -1.07$ in the upper 25 m. Values of N^2 are marginally lower when compared to week 1.

3.4. Summer 2010 surveys

The campaigns of week 4 and 5 were conducted across spring and neap tides, respectively. The combination of the downward-facing ADCP to assess current flow and the MSS to observe the TKE dissipation was again employed, illustrating the contrasts between the two tidal regimes (Figure 10). The dominance of the ebb tide is again prominent in week 4, with peak flow magnitudes occasionally exceeding $0.50\,\mathrm{ms}^{-1}$ between hours four and six. Low water was around hour six, and high water a little before hour 12. In the two hours prior to high water the increase in current magnitude is smaller than that observed shortly before low water, with values here reaching no more than around $0.20\,\mathrm{ms}^{-1}$. There is no direct comparison with week 5 as this survey is conducted over the shorter period of 7 hours. As such, the opportunity to observe the flow regime during the ebb tide is lost. The strongest flow recorded during neap tide is around $0.14\,\mathrm{ms}^{-1}$, shortly before high water during hour 4.

During week 4, ϵ peaks at 10^{-5} $\mathrm{W\,kg}^{-1}$ and unlike the corresponding surveys in spring, at no point exceed this value. There are striking features that mark the evolution of ϵ throughout the tidal cycle here. Broadly, there is a marked discontinuity where a sharp reduction in values of dissipation

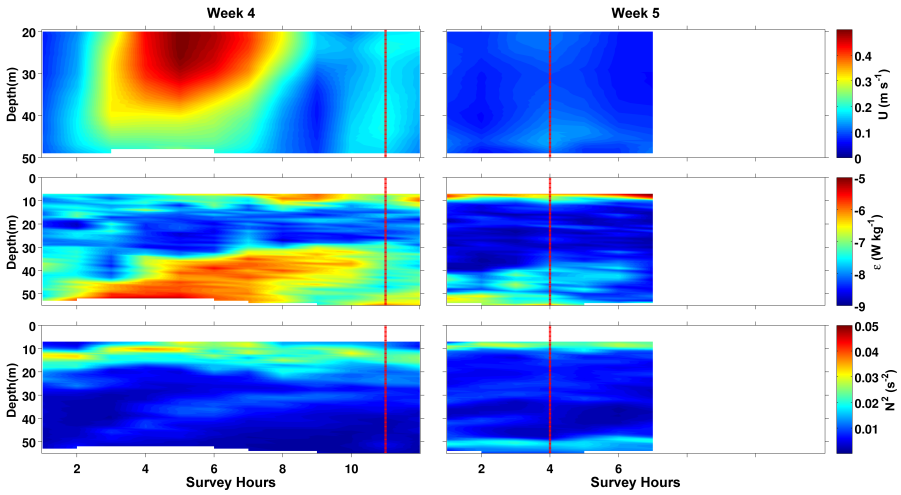

Figure 10: Data from the two surveys of Summer 2010. The top row displays current magnitude (U) from the ADCP, the middle row TKE dissipation (ϵ) with the buoyancy frequency (N^2) comprising the bottom row. The vertical dashed line on each of the plots denotes the time of high water for each survey.

occurs at approximately 30 m, though this is not entirely consistent with the position of the pycnocline which is somewhat shallower at 20 m marked by the peak in N^2 displayed in the lowermost plot of Figure 10, and further highlighted in Figure 11. Week 5 is of course quite different, though there is a noticeable patch of elevated dissipation toward the bed that is sustained throughout much of the duration of this shortened survey. Maximum values of ϵ rarely exceed 10^{-7} W kg^{-1} save for a smaller region close to the bed during the first two hours. The thin region of increased ϵ closer to the surface is most likely due to the transfer of energy from the additional wind and wave activity at the surface.

The depth of the pycnocline is similar to that observed during the week 1 survey in spring 2010. Naturally, the surface to bottom temperature difference is greater, peaking at 4.3 ^{o}C, with the maximum temperature at the surface reaching 16.1 ^{o}C between hours six and eight of the week 4 survey.

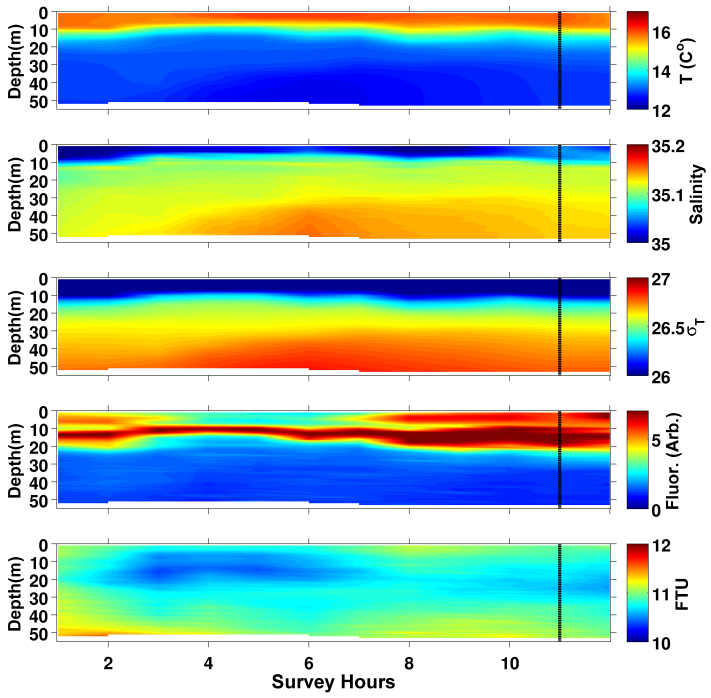

Figure 11: MSS sensor data for week 4. Temperature is the uppermost plot followed by Salinity and σ_T. Fluorescence in arbitrary units to represent relative changes to the sensed voltage follows, with the final plot showing turbidity from the OBS sensor. The vertical dashed line on each of the plots denotes the time of high water for this survey.

This period corresponded with the middle of the afternoon where air temperatures were also at their highest. The plot of density in Figure 11 mirrors that of N^2, denoting a somewhat stronger density gradient present here than seen in the week 1 survey in spring underscoring the influence of seasonal change on the physical regime. Whether L4 can be considered subject to a more permanent thermocline throughout summer is not clear, however, due to the competing forces of temperature and salinity at this location and the propensity for the pycnocline to rapidly erode following increased wind stress or enhanced mixing by tidal forcing. This is further illustrated by the observed picture of the water column presented in Figure 12. Here, the plots of temperature and salinity (and thus density) are much more homogeneous. With temperature, there are thin regions of warmer water at the surface and cooler water at the bottom. Each is of around 5 m in depth, with maximum and minimum temperatures of 15.7 ^{o}C and 13.3 ^{o}C at the surface and bottom respectively. The subsequent reduction in surface to bottom temperature difference of 1.7 ^{o}C implies that thorough mixing has occurred from a combination of the meteorological conditions (Figure 7) and that of the tide.

3.5. Water column energetics

In explaining the temporal evolution of stratification displayed by Figure 9, the potential energy anomaly (PEA) was calculated (following the method outlined by Simpson and Bowers 1981; Simpson et al. 1990 and also more recently by Cheng et al. 2010), to quantify the degree to which L4 is stratified for a given survey and calculate the amount of energy required to bring about a completely mixed water column.

The approach considered by Simpson and Bowers (1981) details the time derivative of PEA, when only stirring by tidal and wind forcing and buoyancy input from solar heating are important. This is also the case for L4, although the extent to which this location is influenced by freshwater outflow from the nearby rivers Tamar and Plym across short time scales is yet to be explicitly quantified. Rainfall for the period of April 2010, as shown in Figure 6, is

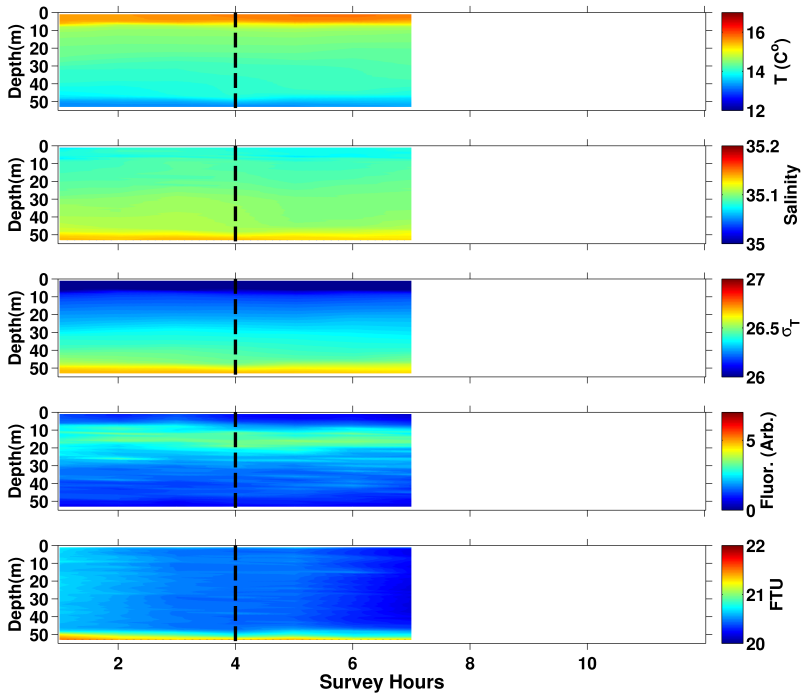

Figure 12: MSS sensor data for week 5. Temperature is the uppermost plot followed by Salinity and σ_T. Fluorescence in arbitrary units to represent relative changes to the sensed voltage follows, with the final plot showing turbidity from the OBS sensor. The vertical dashed line on each of the plots denotes the time of high water for this survey.

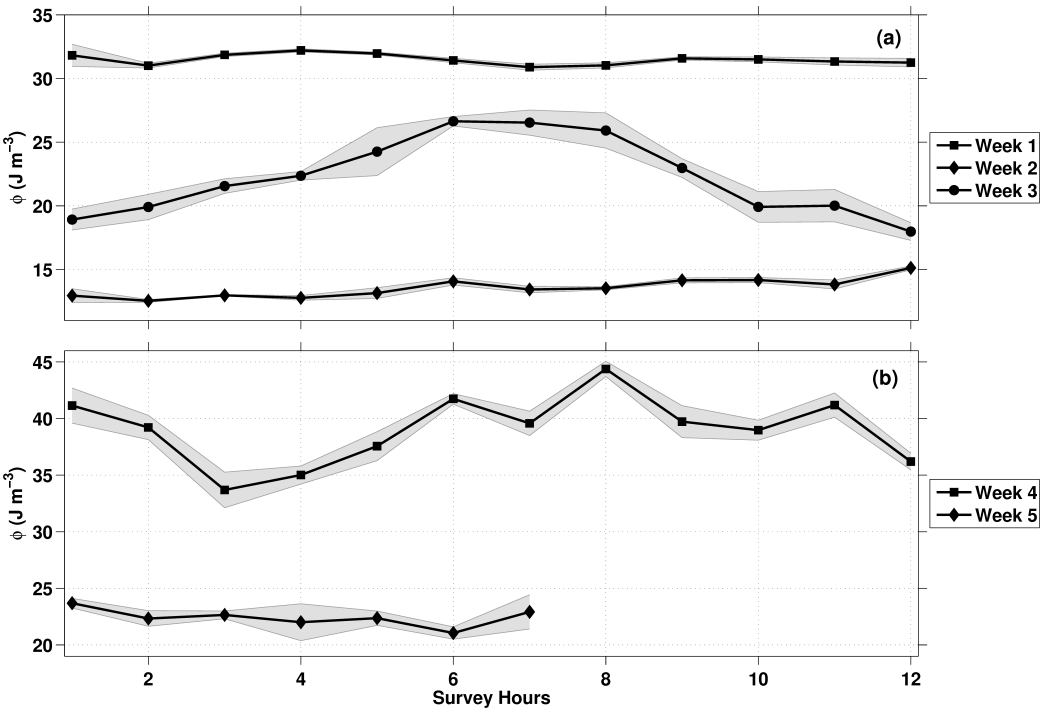

Figure 13: Hourly-averaged Potential Energy Anomaly (PEA) for each of the five surveys. The shaded envelope around the values for each week represent 1 S.D about the mean.

effectively nil so neglecting this as an additional input of buoyancy is valid. Simpson et al. (1990) described the PEA, in units of $\mathrm{J\,m^{-3}}$, as follows:

$$\phi = \frac{1}{H}\int_{-H}^{0}(\bar{\rho}-\rho)\,gz\mathrm{d}z. \tag{4}$$

Here, the overbar defines a depth-averaged value of density, with H representing the total depth of the water column.

The calculated PEA reflects the stratification in each week, with $\phi > 30\,\mathrm{J\,m^{-3}}$ in the spring tide of week 1, $\phi < 15\,\mathrm{J\,m^{-3}}$ for week 2 during neaps. Surface heating is a major contributor to stratification, though despite the increase in surface temperature during week 3 maximum values for ϕ reach only $26.5\,\mathrm{J\,m^{-3}}$, markedly lower than those observed in week 1 (Figure 13a).

Winds were light throughout the spring surveys, and with the corresponding calm conditions it seems likely that during periods when meteorological conditions are less quiescent the PEA will be lower.

The expectation that stratification should be stronger during summer was partially borne-out. As with the spring surveys, though, and in line with the observations displayed in Figures 11 and 12, temporal variability exists between the tidal cycles. Prior to the less favourable meteorological conditions experienced during week 5, it is likely that stratification would have been promoted by light winds and increased levels of solar radiation. This is reflected in the maximum values of PEA of 44.8 $\mathrm{J\,m^{-3}}$, occurring at hour 8 of the week 4 survey in the middle of the afternoon. The mean for the survey is 39.0 $\mathrm{J\,m^{-3}}$. The subsequent mixing and/or presence of advection has reduced the observed PEA for week 5. Here, the maximum value for this curtailed survey is 23.6 $\mathrm{J\,m^{-3}}$ with the mean for the seven hours of data collected being 22.4 $\mathrm{J\,m^{-3}}$. These results compare favourably with those of Groom et al. (2009), who found that in mid-summer L4 values for ϕ were typically in the range of 40-50 $\mathrm{J\,m^{-3}}$.

3.6. Distribution of Plankton populations

3.6.1. Spring surveys

The fluorescence data displays strong signals at particular points in the water column, particularly in the upper layer during weeks 1, 3 and 4. Whether these signals accurately reflect changes to larger plankton can be assessed through the manual counting of individual plankton from the images recorded by the Holocam. The images from the casts of three periods during each survey, the time of high, low and slack water were selected and analysed as per the technique described in section 2 and denoted events A, B and C respectively.

Qualitative assessment of the phytoplankton for all images showed that *Skeletonema* spp., and *Chaetoceros* spp. dominate, examples of which are illustrated in Figure 2. Higher numbers of phytoplankton are recorded during

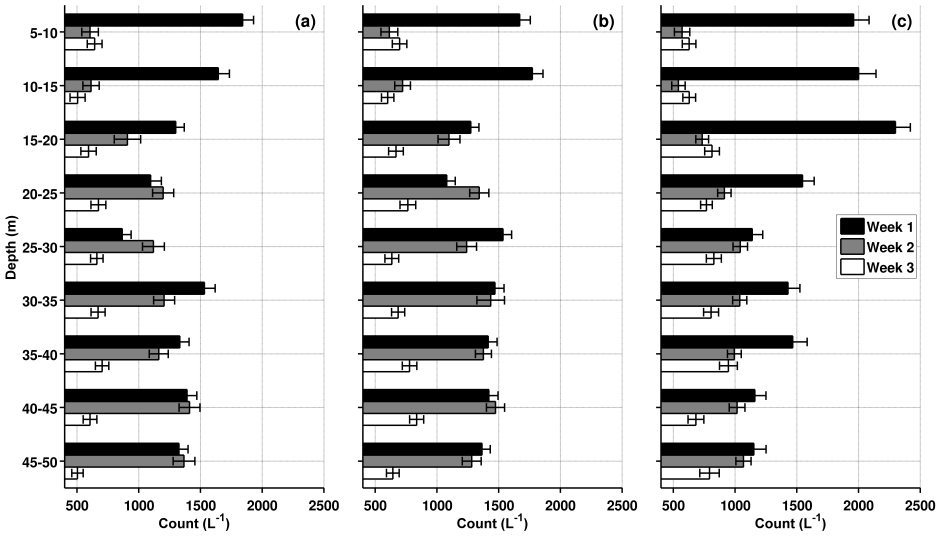

Figure 14: Number counts for the phytoplankton population $\geq 200\,\mu$m during weeks 1, 2 and 3. Plot (a) represents event A, (b) event B and (c) event C for the three surveys.

week 1, and toward the surface in particular where the recorded count is above $1500\,\mathrm{L}^{-1}$ in both of the two uppermost depth intervals throughout the survey (Figure 14). This is not repeated in either of the other surveys, and it is only during week 2 that the count is above $1000\,\mathrm{L}^{-1}$, with counts of around $600\,\mathrm{L}^{-1}$ being more common in week 3. It should be noted here that a single phytoplankton particle according to this classification may comprise of a number of individual cells. Comparisons to other studies that employ cell counts as a measure of phytoplankton biomass have not been conducted.

Event C during week 1 displays counts of phytoplankton that are considerably greater than those of weeks 2 and 3, particularly in the upper 20 m of the water column. At no other point during any of the depth intervals does the count exceed $1500\,\mathrm{L}^{-1}$, perhaps indicating that the values identified during the latter part of the week 1 survey are exceptional. The fluorescence signature for this period reflects the count in the upper three depth intervals (Figure 9). This pattern is not repeated for either the week 2 or 3

survey. The counts for these weeks in the same upper three depth intervals are relatively lower and broadly similar, with counts typically in the region of 500-850 L^{-1}, frequently a factor of two lower than week 1. The consistent domination of diatoms as the most abundant population of larger particles continues at this stage of the tidal cycle for each of the three weeks, although not without a large degree of inter-tidal variability, which is also the case for the other populations under consideration.

The variability demonstrated during the same period for zooplankton is high (Figure 15). The images recorded during week 3 consist of biological particles that are very different in character to either of the previous weeks, as the presence of what are probable examples of jellyfish planula larvae dominate the water column (Figure 16). These plankton are present throughout each of the surveys, but to a lesser extent. The counts for week 1 above 30 m contain no planula, returning a selection of other types of zooplankton (examples of which are shown in Figure 17). Each of the images has been extracted from the full, reconstructed hologram following identification of the particle of interest. Many more of these animals were captured by the Holocam than were returned by WP-2 net trawls throughout the entire sampling period (data provided by the WCO), although it should be noted that the trawls and Holocam casts were not conducted concurrently. The pattern broadly continues for weeks 2 and 3, as the majority of planula are found at depths lower than the pycnocline. In week 3 during the event A period the zooplankton count reaches its maximum of 312 L^{-1} at the 35-40 m depth interval, the depth-averaged value for this point being 196 L^{-1}. This compares to depth-averages of 117 L^{-1} for week 2 and 55 L^{-1} for week 1, illustrating the impact that the increased number of planula have on the total zooplankton population.

For event B, a similar picture is presented. Once more the greatest number of particles are seen during week 3, with counts in excess of 200 L^{-1} for all but the uppermost two depth intervals. There are higher numbers of this

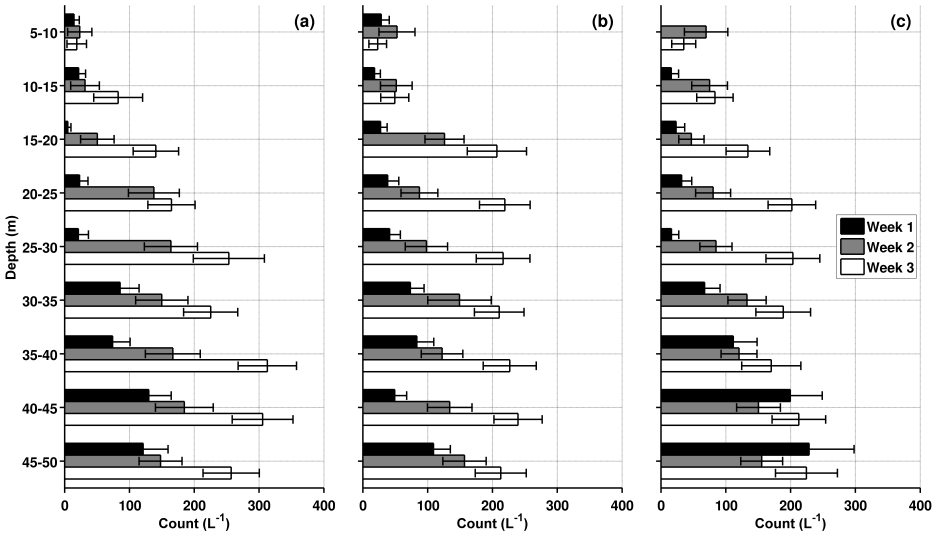

Figure 15: Number counts for the Zooplankton population during April 2010. Plot (a) represents event A, (b) event B and (c) event C for the three surveys.

population present in week 2 when compared to week 1, however for both of these periods counts of less than $150\,\mathrm{L}^{-1}$ are more common. A reflection on the lower number of planula present in week 1, the depth-averaged values here are $52\,\mathrm{L}^{-1}$. This compares to $109\,\mathrm{L}^{-1}$ for week 2 and $178\,\mathrm{L}^{-1}$ for week 3.

The pattern of zooplankton counts with depth exhibited by events A and B continues for the third event, as again numbers of this population increase when below 30 m. Noticeably, however, the maximum number of zooplankton recorded during this event is lower at $228\,\mathrm{L}^{-1}$, which on this occasion is seen at the lowest interval of week 1. For week 2, the zooplankton count does not exceed $160\,\mathrm{L}^{-1}$ and remains relatively stable at the shallower intervals, a feature of this population during this survey across each of the selected events. Overall, and again a reflection of the presence of planula, it is week 3 with the highest depth-averaged values of $162\,\mathrm{L}^{-1}$, compared to $77\,\mathrm{L}^{-1}$ for week 1 and $102\,\mathrm{L}^{-1}$ for week 2.

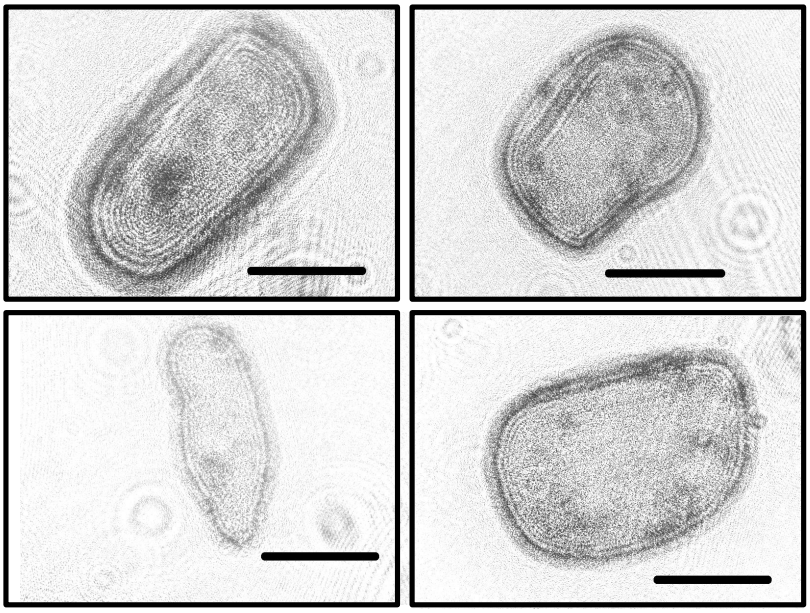

Figure 16: A selection of the probable planula larvae which increased the zooplankton population count in each of the spring surveys, with the scale bar in each image set to 1000 μm. These examples are unreconstructed, normalised raw images. Figure adapted from Cross et al. (2013).

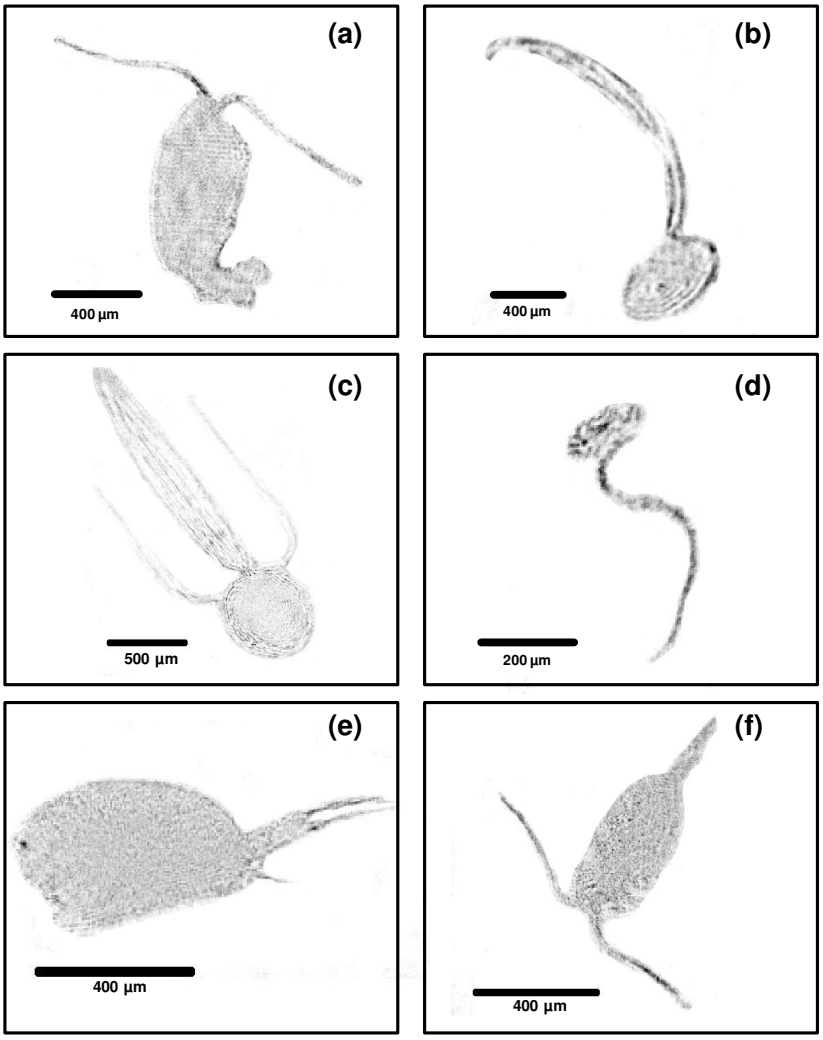

Figure 17: A selection of zooplankton that do not fall into the category of planula. Image (a) shows a copepod; image (b) is a probable example of *Oikopleura* spp.; image (c) an undetermined ascidian larvae; image (d) another example of *Oikopleura* spp. ; image (e) a crustacean larvae; image (f) a further copepod example.

Overall, a lower number of zooplankton are observed which is generally the expectation at L4 given the dominance of phytoplankton, although this may be a function of season. Comparisons to the population counts of the

Table 1: Comparison of depth-averaged counts of zooplankton populations across Weeks 1, 2 and 3.

	WP-2 Planula (L^{-1})	**WP-2 Other (L^{-1})**	**Holocam Planula (L^{-1})**	**Holocam Other (L^{-1})**	**Holocam Total (L^{-1})**
Week 1	0	3.6	47.4	14.0	61.4
Week 2	0	3.7	92.0	17.3	109.3
Week 3	0	2.2	157.2	21.3	178.5
Mean N(L^{-1})±S.D	0 (0)	3.2 (0.76)	98.9 (55.2)	17.5 (3.7)	116.4 (58.9)

WCO assessed by using WP-2 nets for the same period are shown in Table 1. Though there is a lag between the two sampling techniques, differences exist for all three weeks. Eloire et al. (2010) conducted a long-term investigation into zooplankton composition at the L4 site, utilising data from the previous 20 years. The peak in zooplankton population occurs in April, with the average number of zooplankton equating to $4.5\,L^{-1}$ with Copepods making up as many as 90% of this number. With some of the recorded counts in this study indicating a population of many times this, it would appear that the use of a WP-2 net alone may be under-resolving the zooplankton population at L4.

For the Holocam data, Table 1 shows the depth-averaged zooplankton count for the three casts relating to each of the events for weeks 1, 2 and 3. A distinction has been made between Planula larvae and 'other' zooplankton, typically the Copepods or Appendicularians that strongly impact upon the ecosystem dynamics of coastal and shelf sea systems (Gowen et al., 1999; Gallienne and Robins, 2001). This has been done to account for the likely seasonal nature of the planula population, focusing on the zooplankton which are important grazers of phytoplankton and, with respect to the Appendicularians, contributors to particulate organic matter (POM) (Hopcroft

and Roff, 1998). It is unfortunate that concurrent water samples were not obtained alongside the Holocam casts in order to effect a more explicit comparison. However, the recorded number of non-planula zooplankton is consistently above that captured by the WP-2 net by a factor greater than five and the 20 year average for April reported by Eloire et al. (2010) by almost a factor of four. Further, the reported counts are for the region of the water column from 5-50 m, as opposed to the bed to the surface as would be sampled by the WP-2 net. Owing to this artificial shortening of the total sample volume, the depth-averaged Holocam counts shown in Table 1 are likely to under-estimate the total number of zooplankton.

3.6.2. Summer surveys

For weeks 4 and 5, event A represents hours 4 and 1 respectively, with hours 9 and 5 constituting event B. Differences occur for the phytoplankton population, more notably between events A and B of week 4. The relative measure of fluorescence displayed in Figure 11, it is apparent that a similar increase in the phytoplankton population to that observed during week 1 is present. As with week 1, fluorescence increases throughout the survey toward the surface as the survey progresses through the tidal cycle. This is in addition to the marked, elevated region of fluorescence that appears to be consistent with the bottom of the thermocline. Also reflected in the counts, the maximum number of phytoplankton particles exceed $2500\,\mathrm{L}^{-1}$ on two occasions at the 10-15 m and 15-20 m depth intervals during week 4 (Figure 18b). During event A in week 4, the population counts broadly reflect the fluorescence measurement from the MSS, with enhanced counts in excess of $1000\,\mathrm{L}^{-1}$ between 10 and 20 m, before falling considerably below this value as depth increases. A similar pattern exists for week 5, commensurate with the weaker, but nonetheless present, enhanced fluorescence signal at a comparable depth to that of week 4. The same conditions persist for event B, reflected by the counts for this stage of the tide in week 5.

For zooplankton, the variability between weeks 4 and 5 is less marked.

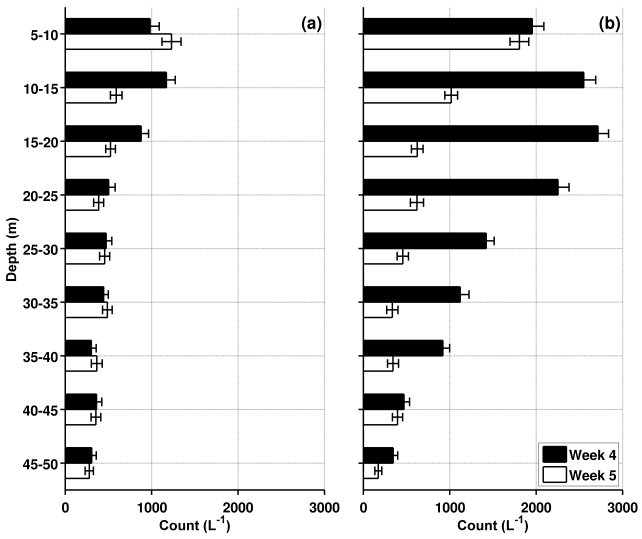

Figure 18: Particle number counts for the Phytoplankton population during July/August 2010. Plot (a) represents event A, and (b) event B for the two surveys.

Of particular note is the absence of the planula larvae that were abundant throughout the Spring surveys of weeks 1, 2 and 3. Thus, the numbers reflected by the counts in Figure 19 represent only those animals illustrated by the examples in Figure 17, that is organisms that are 'hard-bodied' such as the Copepods and Appendicularians. The absence of any zooplankton for a given week or interval is marked by a gap at the appropriate depth bin. The largest value for either week, $45\,\mathrm{L}^{-1}$, is observed during event B in week 4, though most of the recorded counts fall below this yielding depth averaged values of $11.2\,\mathrm{L}^{-1}$ for week 4 and $10.5\,\mathrm{L}^{-1}$ for week 5.

The relatively lower number of zooplankton observed during the summer surveys is closer to the long term average than those of April. The absence of the gelatinous planula is in part responsible for this, though this will now provide a better opportunity to compare with the net trawls of the similar period, given that it is only the harder-bodied organisms that are present.

The comparisons between the two methods are again to be treated with

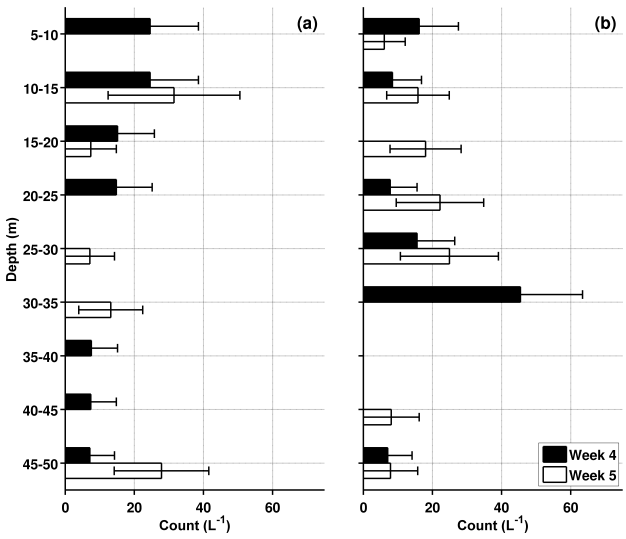

Figure 19: Particle number counts for the Zooplankton population during July/August 2010. Plot (a) represents event A, and (b) event B for the two surveys.

Table 2: Comparison of depth-averaged counts of zooplankton populations across weeks 4 and 5.

	WP-2 count (L^{-1})	**Holocam count (L^{-1})**
Week 4	13.7	11.2
Week 5	5.7	10.5
Mean N(L^{-1}) ± S.D	7.7 (5.3)	11.8 (1.7)

some caution, as the net trawls were conducted two days prior to the tidal station surveys. Table 2 displays the depth-averaged values for both techniques, and in the case of the Holocam counts, the values here represent the average for both of the casts of events A and B. Perhaps surprisingly, given the counts observed during the surveys of April, the WP-2 count for week 4 of 13.7 L^{-1} exceeds that of the Holocam. The monthly average for the 20-year time series considered by Eloire et al. (2010) gives close to 3 L^{-1} for July and around 3.5 L^{-1} for August. Week 5 displays a similar pattern to that seen in weeks 1, 2 and 3, whereby the numbers of zooplankton from the

net trawl is somewhat lower than the counts returned by the Holocam.

4. Discussion

4.1. Physical characteristics of L4

L4, whilst being subjected to many wide-ranging and comprehensive surveys dating back to the early part of the last century, has mainly been a focal point for the study of biological, and to a lesser extent chemical activity. Comprehensive assessment of the physical characteristics of L4, beyond that of 1-D observations of temperature and salinity, are rare. However, the supposition that advection plays a dominant role in the local dynamics of the water column has been previously suggested by Pingree and Griffiths (1977) and more recently at L4 by Cross et al. (2014). This potential for advection at this site, which will generate lateral gradients in density, is invoked as a possible driver of small-scale inhomogeneities at L4. The temporal variability observed here therefore suggests the need for caution when undertaking investigations across short time-scales at this and other similar locations globally. It is acknowledged that the presence of advection and the partitioning of the water column into two layers has restricted the interpretation of the Lagrangian experiment to the upper layer, within which the drogued drifter is located. With respect to the distribution of phytoplankton, the striking changes to this population occur within the upper layer so the emphasis on the importance of advection in modulating the distribution is arguably sound. Less confidence is attributed to advection for the somewhat patchy distribution of zooplankton, though further comment on this is left for the following section.

The picture of the weakest stratification at neap tides is a function of the timing of the surveys. Each survey is a 12-hour snapshot, broadly captured either at the commencement of springs or neaps, therefore leaving little time for the relevant strengths of the tidal forcing to establish control of the vertical structure prior to each campaign. Therefore, there is the appearance

of hysteresis at L4 which is perhaps somewhat misleading as the strongest stratification during the week 1-3 surveys appears at spring tides.

The temperature-dominated survey of week 3 is in contrast to week 1, as illustrated by the density ratio, R_ρ (Figure **??**). The resulting shallower and weaker pycnocline is evidenced by the degree to which a patch of enhanced turbulence is able to breech the pycnocline, possibly transporting nutrients, suspended particles, heat, salt and momentum with it. It has been observed that in temperate shelf seas the onset of stratification in spring can be determined by a combination of the strength of mixing driven by tidal, wind and, to a lesser extent, convective forcing (Sharples et al., 2006; Sharples, 2008). In the absence of any meaningful atmospheric forcing during this period, and given that the strength of the tidal forcing alone is apparently insufficient to entirely overcome the weakly-stratified water column, it is doubtful that mixing is exclusively responsible for the rapid temporal change observed between the three surveys.

Tidal forcing is often considered to be the dominant contributor to mixing at L4 (e.g. Lopez-Urrutia et al. 2005; Lewis and Allen 2009), and this is reasonable in the absence of any previous investigation into the physical drivers of stratification here. Other studies have recognised that quantifying the temporal evolution of stratification as an important part of developing 1-D coastal observatories. This has received less attention when the focus has been on assessing long-term change (which is the principal motivation for their existence), however it has perhaps not been considered that such striking differences can occur over such short time-scales. A recent investigation by Groom et al. (2009) observed that mid-summer values of ϕ at L4 compared poorly with sites in the Celtic Sea for the same season, albeit with measurements taken in the latter location from an earlier period. In acknowledging that L4 should be regarded as only exhibiting weak stratification, and presumably therefore prone to complete mixing from the tidal and atmospheric forcing, it is important to address this potential for variability.

That stratification at L4 never becomes fully established is illustrated well by Figure 13. Mixing between the spring and neap tides for weeks 4 and 5 may have reduced ϕ by half, substantially below the assumed average for the summer noted by Groom et al. (2009). A further campaign following week 5 would have been advantageous in determining whether the water column would re-stratify to the point which is observed during week 4. Spring-neap modulation of the PEA is often associated with more defined regions of freshwater influence, such as Liverpool Bay and the Rhine ROFI (e.g. Fisher et al., 2002; Polton et al., 2011). In this area, where freshwater input is potentially important but less influential, it is assumed that the alternation between high and low vales of PEA is predominantly brought about by the action of the tide. For the most part, these surveys were carried out in the absence of strong meteorological forcing, which will also have the effect of reducing the PEA further.

The sources of the advected properties, in particular the observed salinity structure of week 1, is not altogether certain though one candidate is possibly the freshwater outflow from the River Tamar. As previously noted, the work of Siddorn et al. (2003) modelled the flow from the Tamar and found that the potential exists for freshwater to reach L4. Assuming this has occurred for the week 1 survey, it is particularly striking that it has done so in the absence of any large rainfall events. This suggests that salinity-induced stratification of this kind could well be a regular feature at this location, altering the water column properties on a periodic basis and potentially influencing the exchange of nutrients and suspended particulate matter. Further quantification is necessary here in the form of more intensive observations across longer periods of time, examining the extent of advection from this source. Additional effort must be given to examining the permanency of this variability, in light of the importance of the L4 station in providing time-series observations that assist in identifying ecosystem and climate-related change.

4.2. Plankton distribution

Throughout each of the events within each survey there are contrasts in the phytoplankton counts. During week 1, the pattern of greater numbers down to the depth of 20 m exists for all of the events. During event C, there is a noticeable disparity between the three surveys. It is proposed that spatial variability at L4, brought about by the presence of vertical shear and the resulting advection that follows, is responsible for this rapid increase in phytoplankton. Additionally, the formation of blooms of diatoms such as those most commonly seen during this work would typically take of the order of days, not the few hours across which the increase in number was witnessed here (e.g. Suzuki et al., 2002).

A similar increase in phytoplankton is not seen elsewhere during any of the spring campaigns. The counts in the upper part of the water column at depths above 20 m during weeks 2 and 3 are lower, in the case of the upper two depth intervals by a factor of three. Across each of the selected events for these latter two weeks the pattern is of increasing numbers of phytoplankton with depth at all intervals below the pycnocline. This is perhaps not entirely expected in light of studies focusing on phytoplankton distribution that have both observed and modelled maximum biomass at the base of the thermocline (e.g. Sharples et al., 2001; Ross and Sharples, 2008). However, given the observations here are taken during the onset of stratification, rather than late summer when stratification is stronger as is the case for the Sharples et al. (2001) study, the summer surveys show that this pattern is not typical for L4 across all seasons.

The advantages of multi-cast sampling above point measurements are considerable when attempting to improve estimates of the distribution of plankton populations. There is great importance placed on accurate assessments of plankton in informing models related to the transfer of carbon across the air-sea interface. As shown here, sampling the water column at one point during a given tidal cycle could lead to substantial over or under-estimates

of their number. Whilst the assumption may be that long-term means of population density will account for these short-term fluctuations, if the degree to which this variability is present is unknown, then the margin of error associated with such measurement strategies may need to be revised.

It is important to ensure that a suite of techniques are available when investigating plankton dynamics in the shallow shelf environment. Obvious limitations of the Holocam are that an image is not always able to identify a precise species, or that the camera resolution is insufficient to provide detail on the size range of interest. The advantages of the non-destructive nature of operation though are considerable, and although chain phytoplankton communities can also be disrupted when sampled using nets or bottles, operating the Holocam in conjunction with traditional water sampling will offer more accurate information into the size of plankton populations.

The differences between the number of zooplankton particles observed, in comparison to both the long term average and net trawls conducted across the same period, is largely a result of the inability of the nets to accurately record gelatinous planula. Concerns over the under-representation of WP-2 nets have been previously raised a number of times in the past (Henroth, 1987; Hopcroft et al., 1998), and more recently by Gallienne and Robins (2001), Remsen et al. (2004) and Riccardi (2010). Frequently, these concerns are largely related to the potential for the population of smaller organisms to be under-resolved by using nets. However, with the results presented here it would seem that the problem is not restricted to smaller size classes alone, but throughout a range of sizes, and also by the fact that the counts are only concerned with those particles that are greater than 200 μm. Possible causes preventing nets from adequately sampling zooplankton populations range from avoidance, clogging and destruction of individual organisms. Each of these is somewhat difficult to quantify, though nonetheless seem reasonable in light of the evidence produced here. If the true population of zooplankton is substantially underestimated, then current ecosystem models that rely upon

the accuracy of such data will need to take this uncertainty into account.

The results with respect to the under sampling of zooplankton should be treated with caution. The lack of concurrent sampling ensures that the only comparison can be between the long-term average and the effectively point-sampled casts of the Holocam. Further work is planned to test this more accurately, and will be reported on in due course. However, that the WP-2 nets do not capture a single planula larvae throughout this period is striking. The short-term temporal variability of the zooplankton is considerable, though, and there remains the possibility that at the point in time that the sampling occurred that few, or perhaps none at all were present. What is perhaps more likely, is that the gelatinous nature of the particles themselves has led to their destruction upon capture by the net, which has been previously noted in similar studies using the same sampling methods (Halliday et al., 2001; Warren et al., 2001). The ecological importance of these planula, and the significance of their presence or absence, needs to be given further attention.

The importance of stratification to the existence of planktonic species is well documented, with both the timing of the onset of stratification (Sharples et al., 2006), and also when it becomes established in later months, particularly with respect to continued growth, and access to a favourable light and nutrient climate (Cianelli et al., 2009). Stratification is variable at L4, clearly being continually influenced by advective forces, placing a degree of stress upon each of the organisms through periodic adjustment and/or erosion of the thermocline (Ross and Sharples, 2008). Evidence of the establishment of stronger stratification is shown in Figure 11 for week 4, albeit subsequently undergoing partial erosion observed in the following week (Figure 12). Perhaps in response to the enhanced opportunity for access to nutrients, the concurrent streak of increased fluorescence at the same position of the thermocline during week 5 indicates that species of phytoplankton are present, as has been observed frequently in other shelf sea locations (Sharples

et al., 2001). This suggests that during summer advection may not lead to the wholesale change in water column structure observed in spring over the course of a spring-neap cycle, assuming that the local temperature-salinity field remains similar across spatial scales relative to the tidal excursion.

Throughout the tidal cycle in week 4, the fluorescence signal displays some asymmetry and appears to encompass a wider region of the water column toward the latter part of the survey than at the beginning. This is matched by an equivalent rise in the number of phytoplankton at the same point (Figure 18). For many of the depth intervals, the difference between the two events is striking, as the counts are often a factor of two, and sometimes three, greater than the earlier part of the survey. For the following week 5, albeit only half a tidal cycle, the counts are more homogeneous and the disparity is not present. During week 1, the similar difference was attributed to advection, whereby a larger population was brought into the sampling field by variable current flow in the upper part of the water column, as observed in similar locations (e.g. Hill et al., 2005), and it is likely that the same process occurs for week 4. This further demonstrates the importance of acknowledging that advection at L4 is an active process when assessing inter- and intra-tidal variability. This short term variability in the plankton population is demonstrated by the contrast between the surveys of week 4 and 5. Near the surface, numbers of phytoplankton are similar between the spring and neap tidal cycles, but very quickly the number of phytoplankton falls as depth increases, as implied by the fluorescence signal. Plankton variability across spring-neap cycles in shelf seas has been demonstrated previously (Domingues et al., 2010), further emphasising the need for more frequent sampling to take this into account.

When examining the changes to zooplankton populations, there are notable differences displayed between the seasons, largely in response to the absence of the jellyfish planula. For both surveys in the summer, the count at no time exceeds $50\,\mathrm{L}^{-1}$, considerably lower than the counts observed in spring. In line with the reduction in phytoplankton during summer months,

however, this is perhaps expected and has been shown to occur several times previously (e.g. Coyle and Pinchuk, 2005; Eloire et al., 2010). Once more, the agreement between the results of the Holocam and those of the net counts is poor, although the discrepancy is not as striking as for the earlier surveys. The long term average (around $3.5\,\mathrm{L}^{-1}$) is also supportive of the general trend for the number of zooplankton species to be reduced during this time of year.

5. Conclusions

At present, a range of parameters are collected from the L4 station by either the automated L4 buoy or weekly via research vessel. Both mechanisms are point measurements, yielding useful but limited data as no appreciation is given for how the biological and chemical samples of choice interact with physical forcing. As has been identified by the present study, temporal variability exists with respect to the evolution of stratification and the development of the seasonal pycnocline. In the event that data from this 1-D moored observatory is utilised in investigations of shorter weekly or intra-seasonal activities, the continuing measurement programme may need to address this as an ongoing concern.

The campaigns undertaken for this research were the most comprehensive physical investigation into the mechanics of L4 to date. That L4 is regarded to be weakly-stratified is well understood, but the degree to which the presence of advection might alter the vertical structure of current flow was previously unknown. The process whereby the water column moves from mixed to stratified during spring has been demonstrated to be complex and delayed by inter-tidal variability. The influence of freshwater run-off remains something of an unknown, although it has been shown previously through the long term time series that river outflow does contribute to the salinity structure here. Parcels of water that vary in temperature and salinity are likely to be responsible for altering the density of the water column through advection. The lowered salinity of week 1 is a potential example of this,

though in the absence of any meaningful rain in the weeks leading to that campaign, it is unlikely to have been the river run-off providing the source. The subsequent influence on plankton populations is clear, and the degree to which such changes occur at L4 must now be considered as frequent.

The manual count of the images provided by the Holocam has provided strong evidence for the need to conduct further work in the area of zooplankton identification and enumeration. With respect to phytoplankton, the mechanism used to count these particles is not readily transferred to existing studies, which typically prefer to use a cell count. There is the possibility that individual cells can be counted using the reconstructed images in the same way as for entire colonies of diatom chains. This is, however, likely to be a very time-consuming task and would need to be given thought. A potential solution would be concurrent water sampling, with the traditional method of enumerating cells married to the manual counts, which may provide some indication of the extent to which the two techniques are in agreement.

The requirement for inter-disciplinary studies to increase in number at L4, and at similar 1-D coastal observatories, is clear. Future work at this site may need to be equally well resolved. This is particularly important when identifying the extent to which the presence of temporal variability will impact upon current estimates of the distribution of plankton, and by what margin the difficulty of inter-year comparisons will increase as a result.

6. Acknowledgements

This work was supported by NERC grant (NE/G52388X/1), and also by EU MyOcean (218812) R&D PB-LC 10-103. Many thanks to the crew of the *RV Quest*, to Emlyn Davies, Dan Buscombe and Bob Brewin for additional labour. Thanks also to Dr. Emily Baxter who provided assistance in the identification of the planula larvae.

References

Caley, M.J., Carr, M., Hixon, M., Hughes, T., Jones, G., Menge, B., 1996. Recruitment and the Local Dynamics of Open Marine Populations. Annual Review of Ecology and Systematics 27, 477–500.

Cheng, P., Valle-Levinson, A., Winant, C.D., Ponte, A.L.S., Gutierrez de Velasco, G., Winters, K.B., 2010. Upwelling-enhanced seasonal stratification in a semiarid bay. Continental Shelf Research 30, 1241–1249.

Cianelli, D., Sabia, L., d'Alcala, M.R., Zambianchi, E., 2009. An individual-based analysis of the dynamics of two coexisting phytoplankton species in the mixed layer. Ecological Modelling 220, 2380–2392.

Corcoran, A., Shipe, R., 2011. Inshoreoffshore and vertical patterns of phytoplankton biomass and community composition in Santa Monica Bay, CA (USA). Estuarine Coastal and Shelf Science 94, 24–35.

Coyle, K., Pinchuk, A., 2005. Seasonal cross-shelf distribution of major zooplankton taxa on the northern gulf of alaska shelf relative to water mass properties, species depth preferences and vertical migration behavior. Deep Sea Research II 52, 217–245.

Cross, J., 2012. The Dynamics of Suspended Particles in a Seasonally Stratified Coastal Sea. Ph.D. thesis. University of Plymouth.

Cross, J., Nimmo Smith, W.A.M., Torres, R., Hosegood, P., 2013. Biological controls on resuspension and the relationship between particle size and the Kolmogorov length scale in a shallow coastal sea. Marine Geology 343, 29–38.

Cross, J., Nimmo Smith, W.A.M., Torres, R., Hosegood, P., 2014. The dispersal of phytoplankton populations by enhanced turbulent mixing in a shallow coastal sea. Journal of Marine Systems 136, 55–64.

Davies, E., Nimmo-Smith, W., Agrawal, Y., Souza, A., 2012. Lisst-100 response to large particles. Marine Geology 307-310, 117–122.

Domingues, R., Anselmo, T., Barbosa, A., Sommer, U., Galvao, H., 2010. Tidal variability of phytoplankton and environmental drivers in the freshwater reaches of the Guadiana estuary (SW Iberia). International Review of Hydrobiology 95, 352–369.

Eloire, D., Somerfield, P., Conway, D., Halsband-Lenk, C., Harris, R., Bonnet, D., 2010. Temporal variability and community composition of zooplankton at station L4 in the western channel: 20 years of sampling. Journal of Plankton Research 32, 657–679.

Fisher, N.R., Simpson, J.H., Howarth, M.J., 2002. Turbulent dissipation in the rhine rofi forced by tidal flow and wind stress. Journal of Sea Research 48, 249–258.

Gallienne, C., Robins, D., 2001. Is oithona the most important copepod in the worlds oceans? Journal of Plankton Research 23, 1421–1432.

Gowen, R., McCullough, G., Kleppel, G., Houchin, L., Elliott, P., 1999. Are copepods important grazers of the spring phytoplankton bloom in the western irish sea? Journal of Plankton Research 21, 465–483.

Graham, G., Davies, E., Nimmo-Smith, W., Bowers, D., Braithwaite, K., 2012. Interpreting lisst-100x measurements of particles with complex shape using digital in-line holography. Journal of Geophysical Research 117, C05034.

Graham, G., Nimmo Smith, W.A.M., 2010. The application of holography to the analysis of size and settling velocity of suspended cohesive sediments. Limnology and Oceanography - Methods 8, 1–15.

Groom, S., Martinez-Vicente, V., Fishwick, J., Tilstone, G., Moore, G., Smyth, T., Harbour, D., 2009. The Western English Channel observatory: Optical characteristics of station L4. Journal of Marine Systems 77, 278–295. Workshop on Coastal Observatories - Best Practice in the Synthesis of Long-Term Observations and Models, Liverpool, ENGLAND, OCT 16-19, 2006.

Halliday, N., Coombs, S., Smith, C., 2001. A comparison of lhpr and opc data from vertical distribution sampling of zooplankton in a norwegian fjord. Sarsia 86, 87–99.

Henroth, L., 1987. Sampling and filtration efficiency of two commonly used plankton nets. a comparative study of the nansen net and the unesco wp 2 net. Journal of Plankton Research 9, 719–728.

Herman, A., Beanlands, B., Phillips, E., 2004. The next generation of optical plankton counter: the laser-opc. Journal of Plankton Research 26, 1135–1145.

Hill, V., Cota, G., Stockwell, D., 2005. Spring and summer phytoplankton communities in the chukchi and eastern beaufort seas. Deep Sea Research II 52, 3369–3385.

Hopcroft, R., Roff, J., 1998. Production of tropical larvaceans in kingston harbour, jamaica: are we ignoring an important secondary producer? Journal of Plankton Research 20, 557–569.

Hopcroft, R., Roff, J., Lombard, D., 1998. Production of tropical copepods in kingston harbour, jamaica: the importance of small species. Marine Biology 130, 593–604.

Hosegood, P.J., Gregg, M.C., Alford, M.H., 2008. Restratification of the Surface Mixed Layer with Submesoscale Lateral Density Gradients: Diag-

nosing the Importance of the Horizontal Dimension. Journal of Physical Oceanography 38, 2438–2460.

Jahnke, R., 2010. A Global Synthesis. Springer-Verlag. chapter In: Carbon and Nutrient Fluxes in Continental Margins: A Global Synthesis. pp. 597–615.

Karp-Boss, L., Azevedo, L., Boss, E., 2007. LISST-100 measurements of phytoplankton size distribution: evaluation of the effects of cell shape. Limnology and Oceanography - Methods 5, 396–406.

Lewis, K., Allen, J.I., 2009. Validation of a hydrodynamic-ecosystem model simulation with time-series data collected in the Western English Channel. Journal of Marine Systems 77, 296–311. Workshop on Coastal Observatories - Best Practice in the Synthesis of Long-Term Observations and Models, Liverpool, ENGLAND, OCT 16-19, 2006.

Lopez-Urrutia, A., Harris, R., Acuna, J., Baamstedt, U., Fyhn, H., Flood, P., Gasser, B., Gorsky, G., Irigoien, X., Martinussen, M., 2005. Response of marine ecosystems to global change: Ecological impact of appendicularians. Contemporary Publishing International. chapter in: A comparison of appendicularian seasonal cycles in four contrasting European coastal environments. pp. 255–276.

Lozovatsky, I., Roget, E., Fernando, H., Figueroa, M., Shapovalov, S., 2006. Sheared turbulence in a weakly stratified upper ocean. Deep Sea Research Part I: Oceanographic Research Papers 53, 387–407.

McCandliss, R., Jones, S., Hearn, M., Latter, R., Jago, C., 2002. Dynamics of suspended particles in coastal waters (southern North Sea) during a spring bloom. Journal of Sea Research 47, 285–302. 26th General Assembly of the European-Geophysical-Society, NICE, FRANCE, 2001.

Pingree, R., Griffiths, D., 1977. The bottom mixed layer on the continental shelf. Estuarine and Coastal Marine Science 5, 399–413.

Polton, J., Palmer, M., Howarth, M., 2011. Physical and dynamical oceanography of liverpool bay. Ocean Dynamics 61, 1421–1439.

Remsen, A., Hopkins, T., Samson, S., 2004. What you see is not what you catch: a comparison of concurrently collected net, optical plankton counter, and shadowed image particle profiling evaluation recorder data from the northeast gulf of mexico. Deep Sea Research Part I: Oceanographic Research Papers 51, 129–151.

Riccardi, N., 2010. Selectivity of plankton nets over mesozooplankton taxa: implications for abundance, biomass and diversity estimation. Journal of Limnology 69, 287–296.

Ross, O.N., Sharples, J., 2008. Swimming for survival: A role of phytoplankton motility in a stratified turbulent environment. Journal of Marine Systems 70, 248–262.

Rzadkowolski, C., Thornton, D., 2012. Using laser scattering to identify diatoms and conduct aggregation experiments. European Journal of Phycology 47, 30–41.

See, J., Campbell, L., Richardson, T., Pinckney, J., Shen, R., 2005. Combining new technologies for determination of phytoplankton community structure in the northern gulf of mexico. Journal of Phycology 41, 305–310.

Sharples, J., 2008. Potential impacts of the spring-neap tidal cycle on shelf sea primary production. Journal of Plankton Research 30, 183–197.

Sharples, J., Moore, C., Rippeth, T., Holligan, P., Hydes, D., Fisher, N., Simpson, J., 2001. Phytoplankton distribution and survival in the thermocline. Limonology and Oceanography 46, 486–496.

Sharples, J., Ross, O., Scott, B., Greenstreet, S., Fraser, H., 2006. Inter-annual variability in the timing of stratification and the spring bloom in the North-western North Sea. Continental Shelf Research 26, 733–751.

Siddorn, J., Allen, J., Uncles, R., 2003. Heat, salt and tracer transport in the Plymouth Sound coastal region: a 3-D modelling study. Journal of the Marine Biological Association of the United Kingdom 83, 673–682.

Simpson, J.H., Bowers, D.G., 1981. Models of stratification and frontal movement in shelf seas. Deep Sea Research Part I: Oceanographic Research Papers 28, 727–738.

Simpson, J.H., Brown, J., Matthews, J., Allen, G., 1990. Tidal straining, density currents and stirring in the control of estuarine stratification. Estuaries 13, 125–132.

Suzuki, K., Tsudab, A., Kiyosawac, H., S, T., Nishiokae, J., Sainoa, T., Takahashif, M., Wong, C., 2002. Grazing impact of microzooplankton on a diatom bloom in a mesocosm as estimated by pigment-specific dilution technique. Journal of Experimental Marine Biology and Ecology 271, 99–120.

Warren, J., Stanton, T., Benfield, M., Wiebe, P., Chu, D., Sutor, M., 2001. In-situ measurements of acoustic target strengths of gas-bearing siphonophores. ICES Journal of Marine Science 58, 740–749.

Widdicombe, C.E., Eloire, D., Harbour, D., Harris, R.P., Somerfield, P.J., 2010. Long-term phytoplankton community dynamics in the western English Channel. Journal of Plankton Research 32, 643–655.